Bioorganic & Medicinal Chemistry Letters 21 (2011) 1218–1221

Contents lists available at ScienceDirect

Bioorganic & Medicinal Chemistry Letters

journal homepage: www.elsevier.com/locate/bmcl

Structure and property based design, synthesis and biological evaluation of γ-lactam based HDAC inhibitors

Eunhyun Choi [a], Chulho Lee [a], Jung Eun Park [a], Jeong Jea Seo [a], Misun Cho [a], Jong Soon Kang [b], Hwan Mook Kim [b], Song-Kyu Park [b], Kiho Lee [b], Gyoonhee Han [a,c,*]

[a] Translational Research Center for Protein Function Control, Department of Biotechnology, Yonsei University, Seodaemun-gu, Seoul 120-749, Republic of Korea
[b] Bioevaluation Center, Korea Research Institute of Bioscience and Biotechnology, Yangcheong, Ochang, Cheongwon, Chungbuk 363-883, Republic of Korea
[c] Department of Biomedical Sciences (WCU Program), Yonsei University, Seodaemun-gu, Seoul 120-749, Republic of Korea

ARTICLE INFO

Article history:
Received 14 September 2010
Revised 7 December 2010
Accepted 16 December 2010
Available online 21 December 2010

Keywords:
Histone deacetylase
HDAC
Inhibitor
Isoform
Anticancer
In vitro activity
Docking study
ADME

ABSTRACT

Histone deacetylases (HDACs) are involved in post-translational modification and gene expression. Cancer cells recruited amounts of HDACs for their survival by *epi*-genetic down regulation of tumor suppressor genes. HDACs have been the promising targets for treatment of cancer, and many HDAC inhibitors have been investigated nowadays. In previous study, we synthesized δ-lactam core HDAC inhibitors which showed potent HDAC inhibitory activities as well as cancer cell growth inhibitory activities. Through QSAR study of the δ-lactam based inhibitors, the smaller core is suggested as more active than larger one because it fits better in narrow hydrophobic tunnel of the active pocket of HDAC enzyme. The smaller γ-lactam core HDAC inhibitors were designed and synthesized for biological and property optimization. Phenyl, naphthyl and thiophenyl groups were introduced as the cap groups. Hydrophobic and bulky cap groups increase potency of HDAC inhibition because of hydrophobic interaction between HDAC and inhibitors. In overall, γ-lactam based HDAC inhibitors showed more potent than δ-lactam analogues.

Transcriptional modification on histone controls *epi*-gene expression.[1] Histone acetyltransferase and histone deacetylase are involved and play main roles in theses epigenetic modification. Histone acetyltransferases (HATs) cause hyper-acetylation of histones and leads to transcriptional activation, whereas histone deacetylases (HDACs) suppress gene expression.[2] Hypo-acetylation of histones and proteins are known to be related to many pathogenic mechanisms, especially carcinogenesis. HDACs cause epigenetic suppression of tumor suppressor genes during carcinogenic pathomechanism and are considered as promising targets for treatment of cancer.[3] Many HDAC inhibitors effectively arrest of cancer cell growth and induce apoptosis, which are considers as non-cytotoxic chemotherapeutic agents.[4] Currently, many compounds are in both preclinical development and clinical trials.[5] For examples, US FDA approved SAHA (**1**, Zolinza®, Vorinostat)[6] and depsipeptide (**2**, Istodax®, Romidepsin)[7] for treatment of cutaneous T cell lymphoma (CTCL) in 2006 and 2009, respectively. MGCD0103 (**3**)[8] is a benzamide class of HDAC inhibitor and it inhibits HDAC class I and IV selectively (Fig. 1). In our prior studies, we reported design and synthesis of δ-lactam based HDAC inhibitors (**4**) and their pharmacological evaluation for the potential anti-cancer chemotherapeutic agents. The δ-lactam core HDAC inhibitors showed very good potencies to inhibition of both HDAC enzyme and cancer cell growth in vitro and in vivo experiments.[9]

We also performed docking simulation and 3-dimensional quantitative structure activity relationship (3D QSAR) of these δ-lactam analogues using Discover/Insight II modules and QSAR+/Cerius2 modules.[10,11] The δ-lactam core inhibitors bind well in the active site of HDAC and the result of 3D QSAR rationalize that the big size of core groups are difficult to fit in the narrow tubular hydrophobic pocket of the enzyme. It is also rationalized that the bulky and hydrophobic moiety on cap group showed better HDAC inhibitory activities by stabilizing interaction on the surface of HDAC enzyme with the cap group of the inhibitors. We, however, observed the large cap groups increase lipophilicity (i.e., *c*-log *P*) and lead to decrease the microsomal stability of the molecules.[9a,12] Based on these rationales, a smaller core is suggested as more active than larger one because it fits better in narrow hydrophobic tunnel of the active pocket of HDAC enzyme. Thus, we designed and synthesized γ-lactam analogues for potency as well as microsomal stability, and report here their preliminary biological evaluation.

The synthetic process of γ-lactam analogues is shown in Scheme 1. The secondary amines (**6**) were prepared by N-alkylation of synthetic or commercial amines (**5**) with ally bromide.

* Corresponding author. Tel.: +82 2 2123 2882; fax: +82 2 362 7265.
E-mail address: gyoonhee@yonsei.ac.kr (G. Han).

0960-894X/$ - see front matter © 2010 Elsevier Ltd. All rights reserved.
doi:10.1016/j.bmcl.2010.12.079

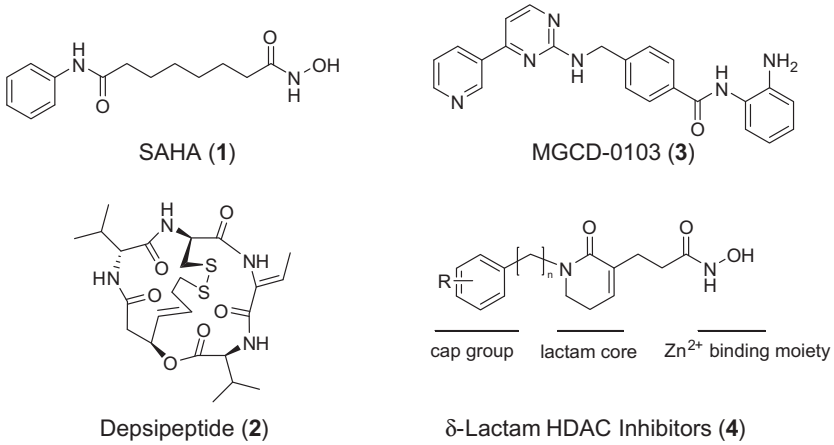

Figure 1. Chemical structures of HDAC inhibitors.

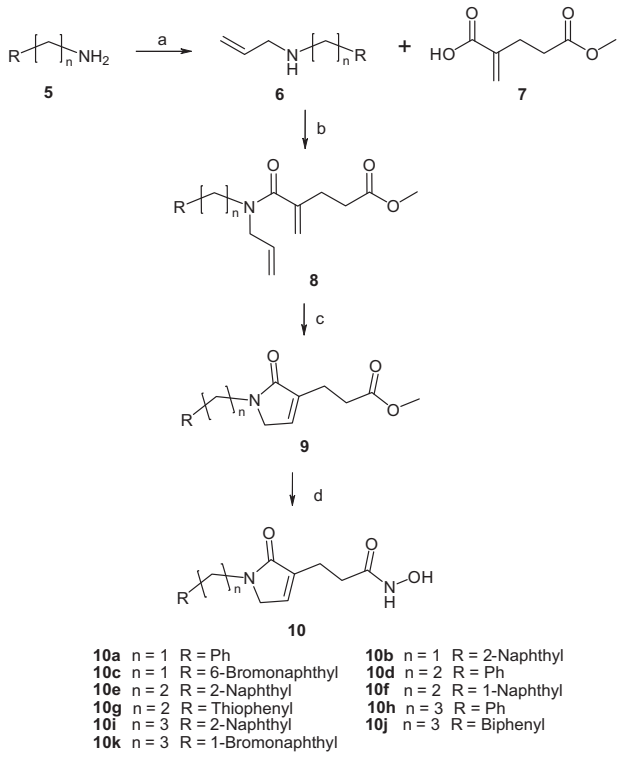

Scheme 1. Reagents and conditions: (a) allyl bromide, hunig's base, CH_3CN; (b) EDC, DMAP, CH_2Cl_2; (c) Grubbs' catalyst (2nd generation), CH_2Cl_2, reflux; (d) $KONH_2$ (1.7 M in MeOH), MeOH, 0 °C.

EDC-medicated coupling of **6** with monoacid **7** afforded amides **8** in good yields. Metathesis reaction of amides **8** with 2–3 mol % of Grubbs' catalyst (the 2nd generation) yielded the γ-lactam rings in high yields. The hydroxamic acid analogues **10** were obtained by reacting with $KONH_2$ in MeOH at low temperature. The prepared γ-lactam analogues differ in carbon chain length between cap group and γ-lactam core by extending from one to three. The phenyl, naphthyl, and thiophenyl moieties were introduced as the cap groups.

All of the prepared γ-lactam analogues were evaluated on HDAC inhibition and cancer cell growth inhibition. HDAC inhibition assay was performed using *HDAC Fluorescent Activity Assay* protocol[13] and cancer cell growth inhibitory activities were evaluated on six human cancer cell lines; PC-3 (prostate), MDA-MB-231 (breast), ACHN (renal), HCT-15 (colon), NCI-H23 (non-small lung cancer), NUGC-3 (gastric) and LOX-IMVI (melanoma). The HDAC inhibition of γ-lactam core inhibitors showed very promising activity at 0.01–0.80 μM in the range of IC_{50} which are better than δ-lactam analogues (Table 1 and Supplementary data). The most of these analogues also showed good cancer cell growth inhibitory activities (GI_{50} = 0.26–10 μM, Table 1). HDAC inhibition of the analogues and their cancer cell growth inhibition are well correlated. Among 6 cancer cell lines, MDA-MB-231 and NUGC-3 cells are more sensitive than others by comparing average GI_{50} values. For the structural rationale toward the activities, the carbon chain length is affected on inhibitory activity; the longer chain is more active than the shorter. The HDAC IC_{50} values of **10a**, **10d** and **10h** are 0.80, 0.12 and 0.05 μM, respectively, and they are 0.15, 0.05, and 0.01 μM for **10b**, **10e** and **10i**, respectively. This may be explained that the structure of active pocket is narrow tunnel as longer chain analogues showed tighter binding to zinc ion and then increase inhibitory activity. Larger naphthyl groups on cap group (**10b**, **10f** and **10i**) are more potent than smaller phenyl group (**10a**, **10d** and **10h**), and 1-naphthyl (**10f**) is less potent than 2-naphthyl (**10e**). These results also explained that larger hydrophobic cap groups show extra stabilizing interaction on the surface of HDAC enzyme. As a result, the hydrophobic and bulky groups on cap group showed good potency. In addition to potent HDAC inhibition, most of these analogues increased acetylation level of histone H3 and H4 in a dose-dependent manner.[9d] For HDAC isoform selectivity, we examined inhibition of HDAC-1, 2, 3, 4 6 and 8 by **10i**, **10j**, **10k** and trichostatin A (TSA), which are highly potent in whole HDAC inhibition. The results of these assays indicated that these analogues inhibited HDAC-6 more than other HDAC isoforms, and HDAC-4 has no direct effect by three synthetic analogues (Table 2). Among 3 compounds, **10i** is most potent and selective to HDAC-6.

The docking study of the most potent inhibitor, **10i** and trichostatin A to the human HDAC-2 (PDB code 3MAX) was performed because **10i** inhibits HDAC-2 at IC_{50} of 16.6 nM which is the second potent among the six HDAC isoforms. Although it inhibits HDAC-6 very potently at IC_{50} of 0.8 nM, no crystal structure of HDAC-6 is available for docking study. The Docked structure of **10i** and HDAC-2 using Discovery Studio is demonstrated in Figure 2.[14] The binding mode of **10i** is similar to that of trichostatin A (TSA); zinc ion in the active site is chelated with hydroxamic acids and cap groups such as naphthyl moiety of **10i** and *N,N*-dimethylaminophenyl group of trichostatin A lies in hydrophobic surface of the enzyme. Furthermore, γ-lactam core of the inhibitor **10i** bound in hydrophobic narrow pocket, which is stabilized by forming

Table 1
HDAC enzyme and cancer cell growth Inhibition by γ-lactam analogues

Compound	IC_{50}[a] (μM)	GI_{50}[a] (μM)						
	HDAC	PC-3	MDA-MB-231	ACHN	HCT-15	NCI-H23	NUGC-3	LOX-IMVI
10a	0.80	30[b]	4.73	30[b]	30[b]	30[b]	NT	30[b]
10b	0.15	4.88	1.22	1.39	3.54	5.19	NT	7.98
10c	0.07	1.16	0.34	NT	0.28	NT	NT	NT
10d	0.12	4.43	0.99	1.08	5.37	4.29	NT	30[b]
10e	0.05	0.34	0.59	0.63	0.84	0.50	0.80	0.61
10f	0.36	5.76	4.76	6.41	6.78	5.13	5.23	3.71
10g	0.30	30[b]	2.86	4.50	9.98	30[b]	NT	30[b]
10h	0.05	3.91	3.81	4.24	6.23	3.46	2.60	4.52
10i	0.01	1.09	0.65	0.65	0.78	0.61	0.61	0.82
10j	0.04	1.41	0.58	0.77	1.14	1.33	0.91	1.16
10k	0.02	0.46	0.52	0.76	1.00	0.26	0.94	0.79
Ave.	0.18	7.95	1.91	6.01	5.99	8.08	1.85	10.96

[a] Values are means of a minimum of three independent experiments. NT: not tested.
[b] GI_{50} = 30 μM represents no activity in 10 μM.

Table 2
HDAC isoform inhibition of **10i**, **10j** and **10k** and trichostatin A

Compound	IC_{50} (nM)					
	HDAC 1	HDAC 2	HDAC 3	HDAC 4	HDAC 6	HDAC 8
TSA	3.9	7.6	5.2	7.690	0.6	73.1
10i	25.6	16.4	80.1	NA[a]	0.8	119.7
10j	76.5	24.0	82.3	NA[a]	6.6	248.6
10k	84.3	23.2	119.8	NA[a]	2.2	331.1

[a] NA: not active.

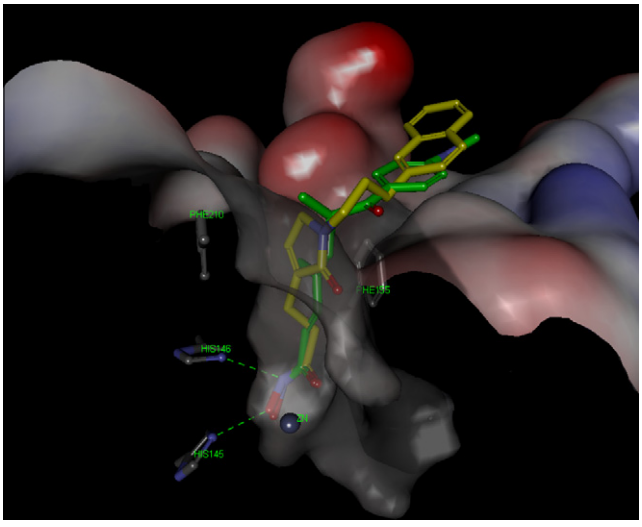

Figure 2. Docked orientation of **10i** (yellow) and TSA (green) to the catalytic site of HDAC-2.

π–π interaction between two aromatic side chains of Phe-145 and Phe-210.

The thiophenyl analogue (**10g**) showed that good HDAC inhibitory activity at 0.050 μM of IC_{50} but its cancer cell growth inhibitory activities are fairly lower compared to the related analogue (**10f**). The polar surface area (tPSA) of **10g** is higher at 97.88, and lipophilicity (log *D*) is lower at 0.19 than other compounds (Table 3). Higher polar surface area and lower lipophilicity may reduce cell permeability and leads to lower inhibition of cancer cell growth. Based on the results of in vitro assays, the inhibitory activities of the prepared γ-lactam analogues are relevant to docking study and QSAR rationale of δ-lactam core HDAC inhibitors.

Table 3
Physicochemical properties of γ-lactam analogues

Compound	Rotatable bond number[a]	tPSA[a]	log *D*[a]
10a	5	69.64	0.43
10b	5	69.64	1.69
10c	5	69.64	2.52
10d	6	69.64	0.59
10e	6	69.64	1.85
10f	6	69.64	1.80
10g	6	97.88	0.19
10h	7	69.64	1.05
10i	7	69.64	2.30
10j	8	69.64	2.67
10k	7	69.64	2.88

[a] PREADME program, BMDRC.[15]

Compound **10i**[16] which showed the best activities of HDAC inhibition and cancer cell growth inhibition was selected for further in vitro and in vivo pharmacokinetic studies. The caco-2 cell permeability of **10i** is good at 16.3 cm/s of $P_{app} \times 10^6$, and the result of metabolic stability indicated **10i** is moderately stable in mouse liver microsomes (Table 4). The caco-2 cell permeability is similar to δ-lactam analogues but the microsomal stability is higher than δ-lactam inhibitors.[8] The pharmacokinetic profiles of **10i** are displayed in Table 5. It showed still high clearance (5.26 l/h/kg), short half-life ($t_{1/2}$ = 0.15, 0.64 h) and low oral bioavailability (*F* = 8.7%). It may be cause by many rotatable bonds and high lipophilicity. The bioavailability of **10i**, however, is better compared to δ-lactam analogue. This rationale is an important consideration for further optimization process.

Finally, in vivo tumor growth inhibitory activity of **10i** using the xenograft experiments was performed. To the female nude mice

Table 4
The caco-2 cell permeability and metabolic stability of **10i**

Compound	Caco-2 cell	% Remaining at 60 min[a]		
	$P_{app} \times 10^6$ (cm/s)	− NADPH	+ NADPH	Buffer
10i	16.3	71.1	43.1	97.2
Negative control	1.5 ± 0.1[b]	96.2[d]	100.8[d]	
Positive control	29.6 ± 0.8[c]	86.8[e]	1.2[e]	

[a] Microsomal stability was determined by incubating 1 μM of test compounds with female ICR mouse liver microsomes (0.5 mg protein/mL) for 60 min at 37 °C.
[b] Ranitidine.
[c] Metoprolol.
[d] Atenolol.
[e] Chlorpromazine.

Table 5
The pharmacokinetics profiles of **10i** in Balb/c mouse

Parameter [a]	Unit	**10i**	
		IV	PO
Dose	(mg/kg)	5	20
T_{max}	(h)	—	0.25
C_{max}	(ng/ml)	—	813
$AUC_{0\text{-}inf}$ [b]	(h ng/ml)	890.2	308.6
CL	(l/h/kg)	5.62	—
V_{ss}	(l/kg)	0.85	—
$t_{1/2}$	(h)	0.15	0.64
F	(%)		8.7

[a] PK parameters were based on mean plasma concentration–time profiles of three animals per time points. PK parameters were calculated by noncompartmental analysis using PK Solutions 2.0 (Summit Research Services, Montrose, CO, USA).
[b] AUC after iv administration was calculated from 0 to infinity, whereas the oral AUC was calculated from 0 to 5 h.

Table 6
In vivo tumor growth inhibition of **10i** in mouse xenograft model

	Dose[a] (mg/kg)	Tumor volume (mm^3)	% Inhibition to the vehicle
Vehicle ($n = 6$)	0	369.8	—
10i ($n = 6$)	30	242.6***	34.4***

[a] Daily treatment (20 days); ip administration.
*** $p < 0.001$.

(seven weeks), HCT-116 (human colorectal cancer) was transplanted (2×10^7 cells/mL). After *intraperitoneal* administration of **10i** at 30 mg/kg for 20 days, it displayed no body weight change and 34.3% of tumor growth inhibition compared to vehicle (Table 6).

In conclusion, based on the SAR and property optimization study of our previous work regarding on δ-lactam based HDAC inhibitors, we designed five-membered γ-lactam core HDAC inhibitors for biological and property optimization. The γ-lactam core has reduced ring size and results in better binding in narrow tunnel of active site. Phenyl, naphthyl and thiophenyl groups were introduced as the cap groups. Hydrophobic and bulky cap groups increase potency of HDAC inhibition because of better hydrophobic interaction between HDAC and inhibitors. The analogues with longer chain length are more active than those with shorter chain. In overall, γ-lactam based HDAC inhibitors showed more potent and are seemed more promising than δ-lactam analogues. The Approach to discovery of a potent compound in vivo experiments and optimization processes for orally active candidate are in progress.

Acknowledgments

This research was supported by National Research Foundation (2009-0092966), Korea Research WCU grant (R31-2008-000-10086-0) and Brain Korea 21 project, Republic of Korea.

Supplementary data

Supplementary data associated with this article can be found, in the online version, at doi:10.1016/j.bmcl.2010.12.079.

References and notes

1. Magic, Z.; Supic, G.; Brankovic-Magic, M. *J. BUON* **2009**, *14*, S79.
2. Pontiki, E.; Hadjipavlou-Litina, D. *Med. Res. Rev.* **2010**.
3. Budillon, A.; Di Gennaro, E.; Bruzzese, F.; Rocco, M.; Manzo, G.; Caraglia, M. *Recent Patents Anticancer Drug Disc.* **2007**, *2*, 119.
4. Kang, M. R.; Kang, J. S.; Han, S. B.; Kim, J. H.; Kim, D. M.; Lee, K.; Lee, C. W.; Lee, K. H.; Lee, C. H.; Han, G.; Kim, H. M.; Park, S. K. *Biochem. Pharmacol.* **2009**, *78*, 486.
5. Tan, J.; Cang, S.; Ma, Y.; Petrillo, R. L.; Liu, D. *J. Hematol. Oncol.* **2010**, *3*, 5.
6. Kavanaugh, S. M.; White, L. A.; Kolesar, J. M. *Am. J. Health Syst. Pharm.* **2010**, *67*, 793.
7. Hymes, K. B. *Clin. Lymphoma Myeloma Leuk.* **2010**, *10*, 98.
8. Prince, H. M.; Bishton, M. J.; Harrison, S. J. *Clin. Cancer Res.* **2009**, *15*, 3958.
9. (a) Yoon, H. C.; Choi, E.; Park, J. E.; Cho, M.; Seo, J. J.; Oh, S. J.; Kang, J. S.; Kim, H. M.; Park, S. K.; Lee, K.; Han, G. *Bioorg. Med. Chem. Lett.* **2010**, *20*, 6808; (b) Kim, H. M.; Lee, K.; Park, B. W.; Ryu, D. K.; Kim, K.; Lee, C. W.; Park, S. K.; Han, J. W.; Lee, H. Y.; Han, G. *Bioorg. Med. Chem. Lett.* **2006**, *16*, 4068; (c) Kim, H. M.; Hong, S. H.; Kim, M. S.; Lee, C. W.; Kang, J. S.; Lee, K.; Park, S. K.; Han, J. W.; Lee, H. Y.; Choi, Y.; Kwon, H. J.; Han, G. *Bioorg. Med. Chem. Lett.* **2007**, *17*, 6234; (d) Kwon, H. K.; Ahn, S. H.; Park, S. H.; Park, J. H.; Park, J. W.; Kim, H. M.; Park, S. K.; Lee, K.; Lee, C. W.; Choi, E.; Han, G.; Han, J. W. *Biol. Pharm. Bull.* **2009**, *32*, 1723.
10. Yang, J. S.; Chun, T. G.; Nam, K. Y.; Han, G., unpublished result.
11. Kim, H. M.; Ryu, D. K.; Choi, Y.; Park, B. W.; Lee, K.; Han, S. B.; Lee, C. W.; Kang, M. R.; Kang, J. S.; Boovanahalli, S. K.; Park, S. K.; Han, J. W.; Chun, T. G.; Lee, H. Y.; Nam, K. Y.; Choi, E. H.; Han, G. *J. Med. Chem.* **2007**, *50*, 2737.
12. Kim, H. M.; Oh, S. J.; Park, S. K.; Han, G.; Kim, K.; Lee, K. S.; Kang, J. S.; Nam, M.; Lee, K. *Xenobiotica* **2008**, *38*, 281.
13. *HDAC Fluorescent Activity Assay/Drug Discovery Kit - AK-500*; BIOMOL® International, Inc.
14. Accelrys, Discovery Studio® 2.5.
15. BMDRC, PREADMET 2.0, Bmdrc, Seoul, Korea, 2007.
16. *N-Hydroxy-3-[1-(3-naphthalen-2-yl-propyl)-2-oxo-2,5-dihydro-1H-pyrrol-3-yl]-propionamide* (**10i**): ^{1}H NMR ($CDCl_3$) δ 10.54 (s, 1H), 7.71 (dd, 3H, J_A = 7.9 Hz, J_B = 6.1 Hz), 7.54 (s, 1H), 7.41–7.33 (m, 2H), 7.22 (s, 1H), 6.64 (s, 1H), 3.69 (t, 2H, J = 7.1 Hz), 3.40 (s, 2H), 2.69 (t, 2H, J = 6.7 Hz), 2.57 (s, 2H), 2.41 (s, 2H), 1.86 (s, 2H); ^{13}C NMR ($CDCl_3$) δ 171.71, 169.96, 138.73, 137.72, 136.65, 133.51, 131.96, 127.90, 127.49, 127.36, 127.03, 126.30, 125.90, 125.16, 50.94, 42.16, 33.16, 31.06, 29.99, 21.98; ESI (m/z) 339.3 (MNa^+).